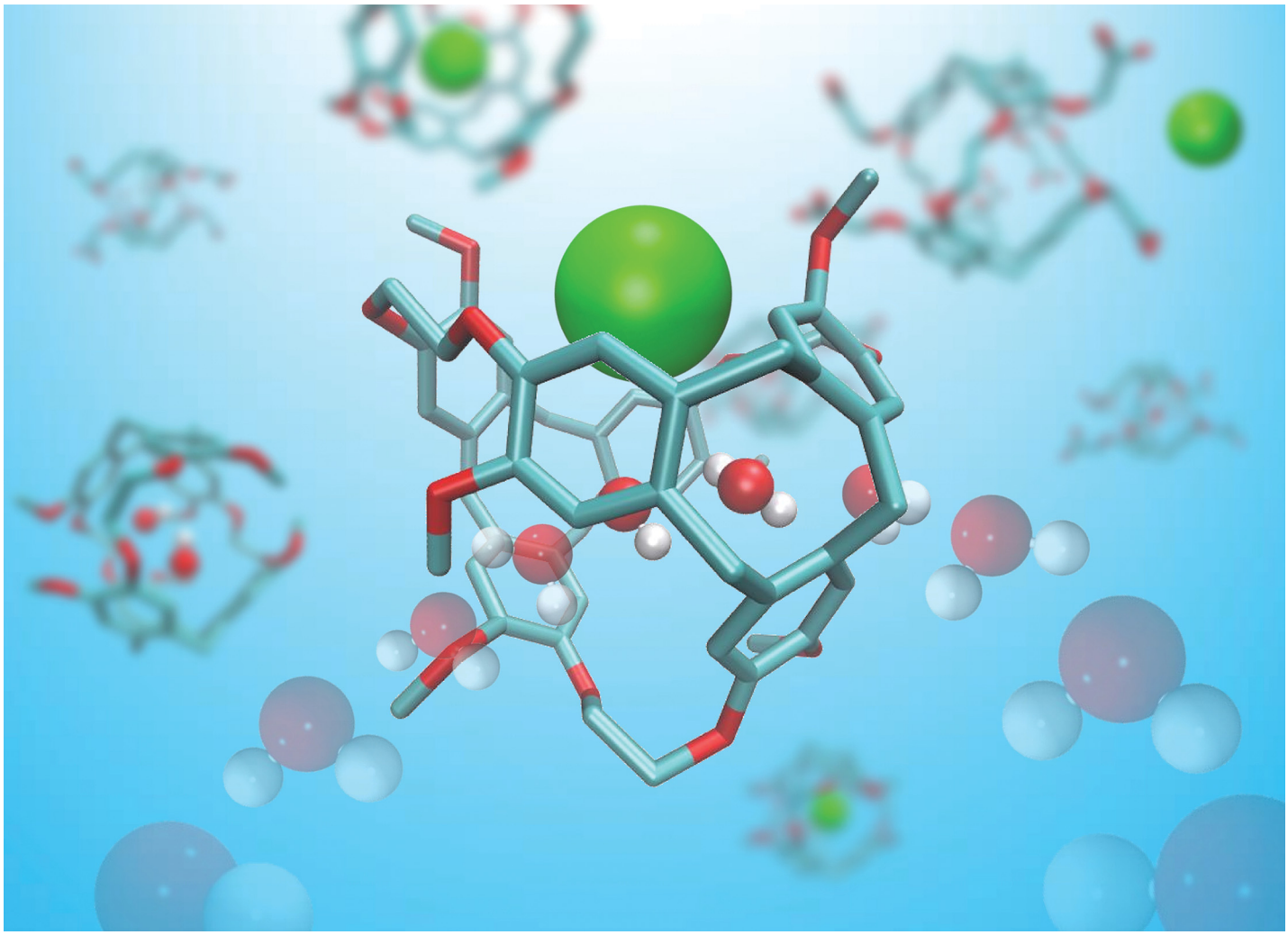

Showcasing research from the NMR Research Unit, University of Oulu, Finland.

Energetics and exchange of xenon and water in a prototypic cryptophane-A biosensor structure

In this work, state-of-the-art semiempirical molecular dynamics and metadynamics simulation methods are applied for the first time to the energetics and dissociation mechanism of a Xe atom between a Xe NMR biosensor cage and aqueous solution. The Xe dissociation pathways, the gating mechanism associated with the cage opening and the role of the in-out exchange of water molecules in initiating the Xe dissociation, are established. This provides detailed microscopic insight into this process that is crucial for the *in vivo* applications of Xe biosensors.

As featured in:

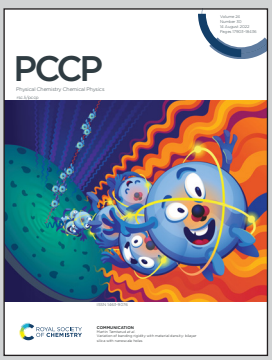

See Perttu Hilla and Juha Vaara, *Phys. Chem. Chem. Phys.*, 2022, **24**, 17946.

ROYAL SOCIETY OF CHEMISTRY

rsc.li/pccp

Registered charity number: 207890

PCCP

ROYAL SOCIETY OF CHEMISTRY

COMMUNICATION

View Article Online
View Journal | View Issue

Cite this: *Phys. Chem. Chem. Phys.*, 2022, **24**, 17946

Received 25th April 2022,
Accepted 13th June 2022

DOI: 10.1039/d2cp01889f

rsc.li/pccp

Energetics and exchange of xenon and water in a prototypic cryptophane-A biosensor structure†

Perttu Hilla * and Juha Vaara

A microscopic description of the energetics and dynamics of xenon NMR biosensors can be experimentally difficult to achieve. We conduct molecular dynamics and metadynamics simulations of a prototypical Xe@cryptophane-A biosensor in an explicit water solvent. We compute the non-covalent Xe binding energy, identify the complexation mechanism of Xe, and calculate the exchange dynamics of water molecules between the solution and the host. Three distinct, hitherto unreported Xe exchange processes are identified, and water molecules initialize each one. The obtained binding energies support the existing literature. The residence times and energetics of water guests are reported. An empty host does not remain empty, but is occupied by water. The results contribute to the understanding and development of Xe biosensors based on cryptophane derivatives and alternative host structures.

Conventional nuclear magnetic resonance (NMR) is troubled by low sensitivity, requiring abundance of the target nuclei in the sample. Xe NMR biosensors[1–4] (XBSs) are microscopic machines capable of molecular recognition at low concentration. The extremely sensitive electron cloud of ^{129}Xe (ref. 5) and the ability to increase the Xe NMR signal intensity by several orders of magnitude[6,7] by hyperpolarization[8] and indirect detection[9,10] enable accurate probing of low-concentration environments. In XBS, the Xe atom is encapsulated in a functionalized host molecule,[1] and introduced as an exogenous agent to the sample. When the host binds to a target molecule with its molecule-selective antenna, a change is reported by the ^{129}Xe NMR chemical shift.[2,3]

Cryptophanes[11–14] (Crs) composed of two linked cyclotriveratrylene (CTV) bowls are currently a favorite category of XBS hosts. Their flexible, roughly spherical cavity is capable of molecular encapsulation *via* van der Waals forces. Crs meet the main requirements for potential hosts:[2] (i) high affinity for Xe and (ii) suitable Xe exchange rate with the solvent. While (i) ensures that a sufficient amount of Xe is encapsulated, (ii) is essential for the Hyper-CEST technique,[6,7] where hyperpolarized Xe enters the host, is depolarized by a frequency-swept irradiation at the resonance frequency in confinement, and is exchanged back to the solution. The resulting decrease of the bulk Xe NMR intensity as a function of the irradiation frequency is used to construct an indirect *z*-spectrum of sufficient intensity.

Host–guest systems are generally significant in chemical sensing and drug design.[15–18] Gaining microscopic information on the non-covalent binding experimentally is challenging. Experiments on the energetics and dynamics of Xe@Cr complexes[7,19–34] initially used an organic solvent.[7,19–23,26,27,30,31,34] The introduction of water solubility-enhancing groups[28] provided increased Xe affinity,[24,25,28,29,32,33] with the Xe guest bound to the water-soluble Cr hosts by *ca.* 5–6 kcal mol^{-1}.

Computational work on Xe@Cr systems includes the Xe chemical shift,[35–40] affinity and dynamics,[38,39,41] structural modifications of the host,[35–38] and role of the solvent.[39–41] The interior volume of the host is decisive for Xe affinity,[14] and a dynamical cage allows an induced fit of the guest.[29] The Xe@Cr binding energy, including some Cr derivatives, is *ca.* 4–17 kcal mol^{-1}.[38,39,41] Many of the studies do not include host dynamics or explicit solvent effects. Dispersion interactions have been found to be essential for these non-covalently bound systems.[38,39,42] In ref. 41, the explicit solvent was found to be important, and correlation between the average number of encapsulated water molecules and Xe affinity was observed.

In this communication we study computationally the host–guest interactions between Xe and the simple, commonly used cryptophane-A (CrA) host, also known as Cr-222, in its natural solvent environment at room temperature. We focus on the Xe binding free energy, ΔA_{Bind}, the mechanism of Xe complexation, as well as the role of solvent water. We attach no targeting or solubility-enhancing moieties, and hence the system can be

NMR Research Unit, P.O. Box 3000, FI-90014 University of Oulu, Finland. E-mail: perttu.hilla@oulu.fi, juha.vaara@iki.fi

† Electronic supplementary information (ESI) available: ESI includes additional material illustrating the basic structure of Cr molecules and explaining the details of system preparation, on chosen MD and MTD parameters, error margin calculations, and numerical computations related to water dynamics are presented. Video examples of three Xe dissociation processes are also included. See DOI: https://doi.org/10.1039/d2cp01889f

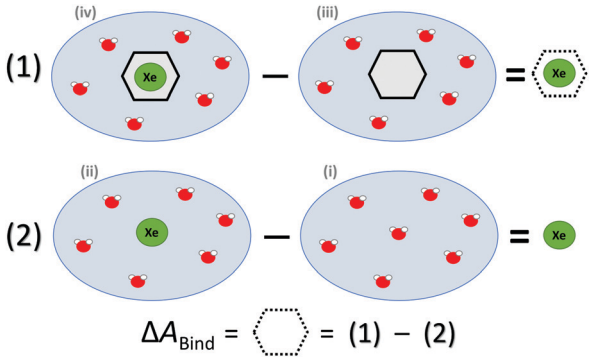

Fig. 1 Thermodynamic cycle of the four sites (see text) simulated to access the free energy of Xe binding to the CrA host, ΔA_{Bind}. Xe atom in green, water molecules in red, CrA cage in black.

viewed as a prototype XBS. Molecular dynamics (MD) and metadynamics (MTD)[43,44] simulations are performed at the semiempirical GFN2[45] and GFN0,[46] as well as at the GFN-FF[47] force-field levels of theory within the *x*TB code.[48,49] The Xe exchange rate between the solution and CrA has been experimentally estimated at *ca.* 10^2 s^{-1} (ref. 2, 3, 20, 21, 32 and 33). Hence, exchange events are rare in the molecular time scale. For this reason, Xe dissociation was modeled by MTD to enhance phase-space sampling. *x*TB employs the density-functional tight-binding approach,[50,51] amenable for configurational and dynamical modeling of non-covalently bound systems over time scales and system sizes exceeding those possible entirely from first principles.

ΔA_{Bind} was estimated by a thermodynamic cycle. Four distinct physical sites (Fig. 1) were simulated: (i) water only, (ii) Xe atom in water, (iii) CrA in water, and (iv) Xe@CrA in water. The averages $\langle E \rangle$ of the total energies of the different sites are subtracted as

$$\Delta E_{Bound} = \langle E_{iv} \rangle - \langle E_{iii} \rangle, \quad (1)$$

$$\Delta E_{Free} = \langle E_{ii} \rangle - \langle E_{i} \rangle. \quad (2)$$

Hence, the free energy of Xe binding becomes

$$\Delta A_{Bind} \approx \Delta E_{Bound} - \Delta E_{Free} \quad (3)$$

The ESI† provides the technical details of the simulations. The results, −4.4 (1.2), −10 (4), and −21 (9) kcal mol^{-1} at the GFN-FF, GFN0, and GFN2 levels, respectively, all reproduce the correct, negative sign of ΔA_{Bind}. The GFN-FF value is in good agreement with prior experiments, *ca.* 5–6 kcal mol^{-1}. The larger ΔA_{Bind} of GFN0 falls in the range of dispersion-corrected density-functional theory (DFT) data and the benchmark MP2 result of ref. 39, while GFN2 agrees with the even stronger binding produced by other DFT functionals.[39] However, it should be noted that the first-principles calculations[39] involved differences of potential energy minima at optimized geometries, whereas the present free-energy differences include the kinetic energy of the atoms. Our GFN-FF datum is expectedly in line with the earlier study[41] that combined force-field MD with free energy perturbation methods. However, moieties increasing the water solubility of CrA, were included in ref. 41. The association constant *K*a and the Eyring–Polanyi exchange rate ω,[52,53]

$$K_a = \frac{1}{c_0} e^{-\Delta A/RT}, \quad (4)$$

$$\omega = \frac{k_B T}{h} e^{-\Delta A/RT} \quad (5)$$

(with c_0 = 1 M) between Xe@CrA and Xe in solution, were calculated with the obtained ΔA_{Bind}. For GFN-FF, GFN0, and GFN2, $K_a = 1.6 \times 10^3$, 2.8×10^7, and 2.7×10^{15} M^{-1}, as well as $\omega = 3.8 \times 10^9$, 2.2×10^5 and 2.4×10^{-3} s^{-1} were obtained, respectively. K_a resulting from GFN-FF is in the best agreement with existing values, *ca.* 10^3–10^4 M^{-1}.[19,21,22,27,28,32,33,41] On the other hand, GFN0 produces the closest order of magnitude for ω (earlier *ca.* 10^2 s^{-1}). eqn (4) and (5) are, however, very sensitive to variations of the exponential factor.

While ΔA_{Bind} and the derived ω are relatively well reproduced by GFN-FF and GFN0, respectively, the GFN2 data appear to be overly attractive. This might be caused by several factors. According to a benchmark study,[42] GFN2 systematically underestimates non-covalent repulsion. Secondly, site (iii) simulation started from an initially empty CrA and, with GFN2, did not proceed to encapsulate any water, unlike with GFN0 and GFN-FF. Presumably the GFN2 trajectory is too short (see ESI†). Hence, $\langle E_{iii} \rangle$ is higher than a system with encapsulated water would have had. This decreases ΔA_{Bind} at the GFN2 level, rendering the host–guest interaction energetically too attractive. Additionally, the lack of solubility-enhancing units in our prototypic XBS can contribute to the discrepancy.

Next, we simulated the dissociation event by using MTD[43,44] to push the Xe atom out from the CrA cavity, in site (iv). The association process would be much harder to simulate in practice, and is assumed to happen *via* the same path. Due to the computational requirements of the semiempirical methods, a sufficient number of long enough MTD simulations with GFN0/GFN2 was out of reach. Altogether, six of the MTD runs performed with GFN-FF produced dissociation, and always in two successive steps: (1) One or more H_2O molecules enter the host cage and co-exist with Xe for a few ps, and (2) Xe exits, leaving one or more encapsulated waters behind. It is, hence, evident that water molecules play a crucial role in the Xe exchange. As expected, both the Xe guest and the water molecules are found to exit (and the H_2O also enter) the cage *via* the portals between the three linkers (Fig. S1 in ESI†). In more detail, the simulated events can be classified into three categories (Fig. 2): (i) A water molecule enters, followed by the displacement of Xe. (ii) Two H_2Os enter from different portals, followed by Xe exiting *via* the third portal. (iii) Two waters enter, one of them travels through the cage, and the other exits through the same portal it entered from. Two *new* waters enter, after which Xe exits as in (ii). Animations of the processes (i–iii) can be found in the ESI.†

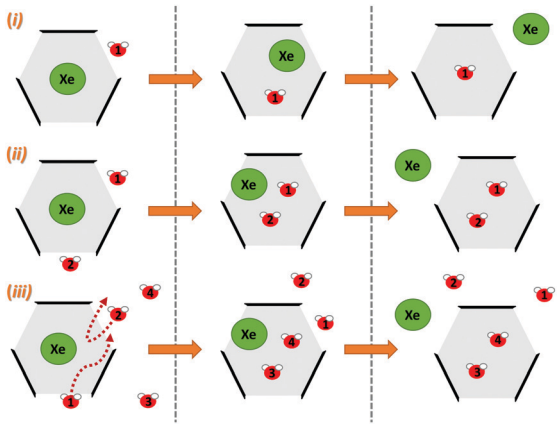

Fig. 2 Three distinct Xe exit processes from CrA, each initialized by inclusion of water molecule(s) that displace Xe.

In each process, the H_2O molecules initialize the rare event, acting like a catalyst. The dissociation is analogous to a single displacement reaction. A schematic pathway of the process (ii) is presented in Fig. 3. Similar graphs on (i) and (iii) are shown in the ESI.† The conformation of the host changes in the Xe dissociation in a combination of the *French door* and *sliding door* gating mechanisms[54] that open/close the portal. In the French door part (grey arrows in Fig. 3, top), the two OCH_3 groups rotate away from the Xe dissociation pathway. In the sliding door part (grey dashed lines), the entire host structure opens by stretching the linkers that connect the CTV bowls.

As Xe displacement is associated with the inclusion of water molecules, the energetics and dynamics of H_2O in site (iii) were further simulated by MD. With GFN0 and GFN-FF, an initially empty, solvated CrA cage does not remain empty, but is eventually occupied by water molecules that undergo fast in-out exchange with the solution. At the GFN2 level this exchange was not observed (*vide supra*). The RMS distances of H_2O molecules from the center of the host illustrate the exchange

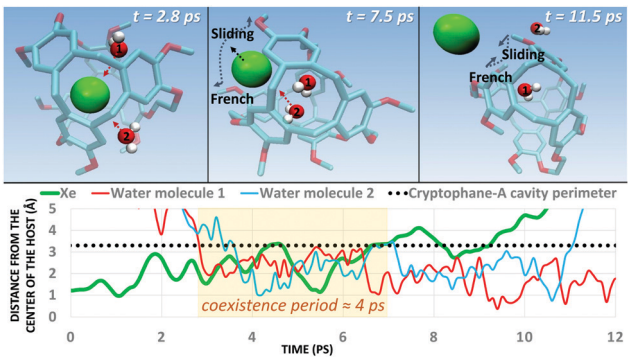

Fig. 3 (Top) Type (ii) Xe dissociation event (see text) from the CrA host, followed by a water molecule exiting. The grey arrows and dashed lines denote the gating mechanism involved. (Bottom) Distance of the Xe atom and the H_2O molecules from the center of the host cage against the MTD time it takes for the process to complete. A coexistence period, where water and Xe reside simultaneously in the cavity, is highlighted in orange. H atoms of the host are not shown for clarity.

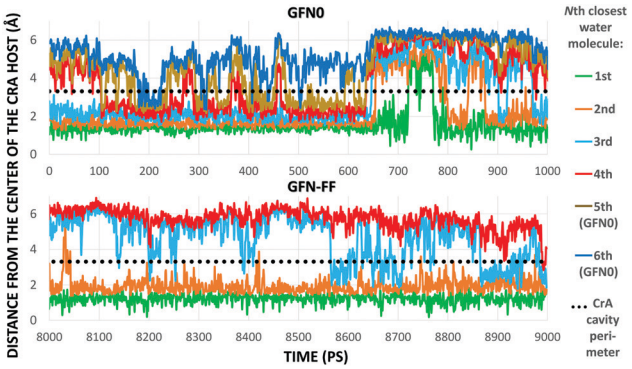

Fig. 4 Distances from the center of the host to the closest water molecules, based on the GFN0 (top) and GFN-FF (bottom) MD simulations. The entire production period (GFN0) or the last ns (GFN-FF) is shown.

(Fig. 4). At the GFN0 level, the CrA cavity is occupied by at least three waters almost throughout the simulation. After *ca.* 700 ps, a short period of empty cavity is also seen. The exchange is markedly slower at the GFN-FF level. The host encapsulates an average of 3.32 and 2.25 water molecules at the GFN0 and GFN-FF levels, respectively.

The distribution of different cage occupation numbers N_W is presented in Table 1. With GFN0, the broad distribution peaks around $3\cdots5$ water molecules, never exceeding six. In contrast, the GFN-FF occupation peaks sharply at 2, with the maximum $N_W = 4$. After the initial equilibration there is always at least one H_2O guest in the CrA cage at this level.

In a two-state system, the relative binding energy ΔA_{BA} between the two states can be approximated by

$$\Delta A_{BA} \approx -RT \ln \frac{N_B}{N_A}, \quad (6)$$

where N_B and N_A are the state populations. Assigning state B as cage occupation $N_W = 0/1$ for GFN0/GFN-FF, leads to the H_2O binding energies with CrA listed in Table 1. The values are approximate due to the finite length of particularly the GFN0 production simulation. With GFN0, the obtained relative binding energy between the smallest ($N_W = 0$) and the most common ($N_W = 3\cdots5$) occupations is *ca.* -1 kcal mol^{-1}. Correspondingly, the energy between the smallest ($N_W = 1$) and the most common ($N_W = 2$) occupation with GFN-FF is *ca.* -2 kcal mol^{-1}. At the

Table 1 Simulated number of water molecules N_W inside the CrA cage. The relative energies ΔA [eqn (6)] refer to $N_W = 0$ and 1 for the GFN0 and GFN-FF levels, respectively. The activation energy normalized by the number of guests, $\Delta A/N_W$, is also shown

		Number of water molecules N_W						
		0	1	2	3	4	5	6
GFN0	RO (%)[a]	4.5	11.9	12.3	24.4	17.2	24.6	5.2
	ΔA[b]	0	−0.58	−0.60	−1.01	−0.80	−1.02	−0.09
	$\Delta A/N_W$[b]	0	−0.58	−0.30	−0.34	−0.20	−0.20	−0.02
GFN-FF	RO (%)[a]	—	2.3	71.8	24.8	1.2	—	—
	ΔA[b]	—	0	−2.06	−1.43	0.38	—	—
	$\Delta A/N_W$[b]	—	0	−1.03	−0.48	0.10	—	—

[a] Relative occupation. [b] In units of kcal mol^{-1}.

GFN0 level, the energetic advantage of adding water guests persists up to $N_W = 6$, where $\Delta A \approx 0$. The largest energy gain, $\Delta A/N_W$, occurs when a single water molecule enters an empty host. With GFN-FF, introducing one water to an already singly occupied host results in the highest energy gain. As $N_W = 0$ did not occur during the entire 8.5 ns production period, it appears to be extremely beneficial to include 1–2 water molecules at the GFN-FF level.

The exchange between encapsulated and bulk water molecules was studied by computing the survival probability function, $P(t)$, of water inside the host. $P(t)$ is the time correlation function of the number of molecules that remain in the cavity after the time t, with the value $P(0)$ equaling the average occupation number. We approximate the mean residence time τ of water molecules through a single-exponential fit to $P(t) \approx P(0)e^{-\frac{t}{\tau}}$, as detailed in the ESI.† The results, τ = 198 (5) and 308 (8) ps at the GFN0 and GFN-FF levels, respectively, are consistent with the in-out exchange behavior of water (Fig. 4) and with the distribution of N_W (Fig. S5, ESI†). Earlier force-field MD simulations[41] for water-soluble CrA derivatives indicate a faster exchange by about one order of magnitude. The underlying force field used in ref. 41 is different from the present *x*TB Hamiltonians. Additionally, our prototypic CrA does not have the solubility enhancing moieties.

Conclusions

In summary, the behavior of a prototypic Xe biosensor, Xe@CrA, in an aqueous medium was studied by MD and MTD simulations. The correct, attractive sign for the Xe binding free energy could be reproduced in a thermodynamic cycle calculation. The binding energies agree well with earlier data, apart from a too attractive result obtained at the semiempirical GFN2 level. MTD simulations enabled the complexation mechanism and pathway of Xe to be identified for the first time. Three qualitatively different processes, each initialized by the inclusion of H_2O molecules, were found. The host conformation changes prior to Xe dissociation in a combination of the French door and sliding door gating mechanisms. There might exist other possible exchange mechanisms, which could not be reproduced in the present, finite set of simulations. Despite the hydrophobic nature of the CrA interior, in an aqueous medium the host cavity is, on average, inhabited by 2–3 H_2O molecules.

Many of the earlier computational studies on XBSs were performed *in vacuo* and/or with static models, omitting the important dynamical and solvent effects modelled here. The present work sheds light on the microscopic description of the solvated Xe@CrA XBS core, supports the existing literature on the thermodynamics of the system, and paves the way for further studies. In addition, MTD is a promising method for the generation of non-covalent host–guest binding events that are out of reach for classical MD.

Author contributions

P. Hilla was responsible for data curation, general investigation, software coding, visualisation of methods and results, and writing of the original draft; J. Vaara supervised the entire work. Both authors contributed together to conceptualisation of the project and reviewing/editing of the manuscript.

Conflicts of interest

There are no conflicts to declare.

Acknowledgements

Drs. V. -V. Telkki and P. Lantto, as well as Mr P. Mayorga Delgado (Oulu) are thanked for many useful discussions. We acknowledge funding from the Academy of Finland (Grant 331008) and U. Oulu (Kvantum Institute). Computations were carried out at CSC–the Finnish IT Centre for Science and the Finnish Grid and Cloud Infrastructure project (persistent identifier urn:nbn:fi:research-infras-2016072533).

Notes and references

1 M. Spence, S. Rubin, I. Dimitrov, J. Ruiz, D. Wemmer, A. Pines, S. Qin Yao, F. Tian and P. G. Schultz, *Proc. Natl. Acad. Sci. U. S. A.*, 2001, **98**, 10654–10657.
2 P. Berthault, G. Huber and H. Desvaux, *Progr. NMR Spectrosc.*, 2009, **55**, 35–60.
3 L. Schröder, *Phys. Med.*, 2013, **29**, 3–16.
4 S. Zemerov and I. Dmochowski, *RSC Adv.*, 2021, **11**, 7693–7703.
5 B. Goodson, *J. Magn. Reson.*, 2002, **155**, 157–216.
6 L. Schröder, T. Lowery, C. Hilty, D. Wemmer and A. Pines, *Science*, 2006, **314**, 446–449.
7 M. Kunth, C. Witte and L. Schröder, *J. Chem. Phys.*, 2014, **141**, 1–9.
8 T. Walker and W. Happer, *Rev. Mod. Phys.*, 1997, **69**, 629–642.
9 K. Ward, A. Aletras and R. Balaban, *J. Magn. Reson.*, 2000, **143**, 79–87.
10 E. Harel, L. Schröder and S. Xu, *Annu. Rev. Anal. Chem.*, 2008, **1**, 133–163.
11 J. Gabard and A. Collet, *J. Chem. Soc., Chem. Commun.*, 1981, **21**, 1137–1139.
12 T. Brotin and J.-P. Dutasta, *Chem. Rev.*, 2009, **109**, 88–130.
13 T. Brotin, A. Martinez and J.-P. Dutasta, in *Calixarenes and Beyond*, ed. P. Neri, J. Sessler and M.-X. Wang, Springer, 2016, pp. 525–557.
14 G. El-Ayle and K. Travis, in *Comprehensive Supramolecular Chemistry II*, ed. J. Atwood, Elsevier, 2017, pp. 199–249.
15 J. Rebek, *Angew. Chem., Int. Ed.*, 2005, **44**, 2068–2078.
16 M. Liu, L. Zhang and T. Wang, *Chem. Rev.*, 2015, **115**, 7304–7397.
17 S. Barrow, S. Kasera, M. Rowland, J. del Barrio and O. Scherman, *Chem. Rev.*, 2015, **115**, 12320–12406.
18 L. Yang, X. Tan, Z. Wang and X. Zhang, *Chem. Rev.*, 2015, **115**, 7196–7239.
19 K. Bartik, M. Luhmer, J.-P. Dutasta, A. Collet and J. Reisse, *J. Am. Chem. Soc.*, 1998, **120**, 784–791.

20 T. Brotin, A. Lesage, L. Emsley and A. Collet, *J. Am. Chem. Soc.*, 2000, **122**, 1171–1174.
21 T. Brotin, T. Devic, A. Lesage, L. Emsley and A. Collet, *Chem. – Eur. J.*, 2001, **7**, 1561–1573.
22 T. Brotin and J.-P. Dutasta, *Eur. J. Org. Chem.*, 2003, 973–984.
23 M. Spence, J. Ruiz, S. Rubin, T. Lowery, N. Winssinger, P. Schultz, D. Wemmer and A. Pines, *J. Am. Chem. Soc.*, 2004, **126**, 15287–15294.
24 G. Huber, T. Brotin, L. Dubois, H. Desvaux, J.-P. Dutasta and P. Berthault, *J. Am. Chem. Soc.*, 2006, **128**, 6239–6246.
25 A. Hill, Q. Wei, R. Eckenhoff and I. Dmochowski, *J. Am. Chem. Soc.*, 2007, **129**, 9262–9263.
26 H. Fogarty, P. Berthault, T. Brotin, G. Huber, H. Desvaux and J.-P. Dutasta, *J. Am. Chem. Soc.*, 2007, **129**, 10332–10333.
27 G. Huber, L. Beguin, H. Desvaux, T. Brotin, H. Fogarty, J.-P. Dutasta and P. Berthault, *J. Phys. Chem. A*, 2008, **112**, 11363–11372.
28 A. Hill, Q. Wei, T. Troxler and I. Dmochowski, *J. Am. Chem. Soc.*, 2009, **131**, 3069–3077.
29 O. Taratula, A. Hill, N. Khan, P. Carroll and I. Dmochowski, *Nat. Commun.*, 2010, **1**, 148.
30 R. Fairchild, A. Joseph, T. Holman, H. Fogarty, T. Brotin, J.-P. Dutasta, C. Boutin, G. Huber and P. Berthault, *J. Am. Chem. Soc.*, 2010, **132**, 15505–15507.
31 Y. Bai, A. Hill and I. Dmochowski, *Anal. Chem.*, 2012, **84**, 9935–9941.
32 S. Korchak, W. Kilian and L. Mitschang, *Chem. Commun.*, 2015, **51**, 1721–1724.
33 S. Korchak, W. Kilian, L. Schröder and L. Mitschang, *J. Magn. Reson.*, 2016, **265**, 139–145.
34 P. Berthault, C. Boutin, E. Léonce, E. Jeanneau and T. Brotin, *ChemPhysChem*, 2017, **18**, 1561–1568.
35 D. Sears and C. Jameson, *J. Chem. Phys.*, 2003, **119**, 12231–12244.
36 J. Ruiz, D. Sears, A. Pines and C. Jameson, *J. Am. Chem. Soc.*, 2006, **128**, 16980–16988.
37 A. Bagno and G. Saielli, *Chem. – Eur. J.*, 2012, **18**, 7341–7345.
38 E. Dubost, J.-P. Dognon, B. Rousseau, G. Milanole, C. Dugave, Y. Boulard, E. Léonce, C. Boutin and P. Berthault, *Angew. Chem., Int. Ed.*, 2014, **53**, 9837–9840.
39 T. Demissie, K. Ruud and J. Hansen, *J. Phys. Chem. A*, 2017, **121**, 9669–9677.
40 E. Léonce, J.-P. Dognon, D. Pitrat, J.-C. Mulatier, T. Brotin and P. Berthault, *Chem. – Eur. J.*, 2018, **24**, 6534–6537.
41 L. Gao, W. Liu, O.-S. Lee, I. Dmochowski and J. Saven, *Chem. Sci.*, 2015, **6**, 7238–7248.
42 K. Kříž, M. Nováček and J. Řezáč, *J. Chem. Theory Comput.*, 2021, **17**, 1548–1561.
43 A. Laio and F. Gervasio, *Rep. Progr. Phys.*, 2008, **71**, 1–22.
44 A. Barducci, M. Bonomi and M. Parrinello, *Wiley Interdiscip. Rev.: Comput. Mol. Sci.*, 2011, **1**, 826–843.
45 S. Grimme, S. Ehlert and C. Bannwarth, *J. Chem. Theory Comput.*, 2019, **15**, 1652–1671.
46 P. Pracht, E. Caldeweyher, S. Ehlert and S. Grimme, *ChemRxiv: A Robust Non-Self-Consistent Tight-Binding Quantum Chemistry Method for large Molecules*, 2019.
47 S. Spicher and S. Grimme, *Angew. Chem., Int. Ed.*, 2020, **59**, 15665–15673.
48 C. Bannwarth, E. Caldeweyher, S. Ehlert, A. Hansen, P. Pracht, J. Seibert, S. Spicher and S. Grimme, *Wiley Interdiscip. Rev.: Comput. Mol. Sci.*, 2020, **11**, e01493.
49 *GitHub: xTB*, **https://github.com/grimme-lab/xtb**.
50 J. Harris, *Phys. Rev. B: Condens. Matter Mater. Phys.*, 1985, **31**, 1770–1779.
51 P. Koskinen and V. Mäkinen, *Comput. Mater. Sci.*, 2009, **47**, 237–253.
52 H. Eyring, *J. Chem. Phys.*, 1935, **3**, 107–115.
53 M. Evans and M. Polanyi, *Trans. Faraday Soc.*, 1935, **31**, 875–894.
54 K. Houk, K. Nakamura, C. Sheu and A. Keating, *Science*, 1996, **273**, 627–629.